Proceedings of the 17th World Congress
The International Federation of Automatic Control
Seoul, Korea, July 6-11, 2008

Optimization of Global Chassis Control Variables

Josip Kasac*, Josko Deur*, Branko Novakovic*,
Matthew Hancock, Francis Assadian****

* University of Zagreb, Faculty of Mech. Eng. & Naval Arch., Zagreb, Croatia
(e-mail: josip.kasac@fsb.hr, josko.deur@fsb.hr, branko.novakovic@fsb.hr).
** Jaguar Cars Ltd, Whitley Engineering Centre, Coventry, UK
(e-mail: mhancoc1@jaguar.com, fassadia@ford.com).

Abstract: The paper presents a global chassis control (GCC) optimization approach using a gradient-based optimal control algorithm. The goal is to find optimal actions of various actuators such as active steering and active differential, which ensure satisfying the optimization criterion (e.g. trajectory following error minimization) subject to different equality and inequality constraints on state and control variables. The optimization algorithm is based on an exact gradient method, where the cost function gradient is calculated by using a backpropagation-through-time-like algorithm. The proposed GCC optimization approach is illustrated on an example of double lane change maneuver using rear active steering and/or rear active differential actuators.

1. INTRODUCTION

The traditional vehicle dynamics control systems based on brake interventions are being improved by introducing new vehicle dynamics actuators such as active steering systems and active differentials. The addition of new actuators opens significant opportunities of improving vehicle active safety and handling performance. However, the overall vehicle dynamics control system becomes a complex multi-input multi-output system (denoted here as Global Chassis Control (GCC) System), which calls for application of modern control techniques to reach the optimal performance.

The GCC system optimization usually relates to finding optimal parameters of a state variable controller (Hancock, 2006) for a linearized vehicle dynamics model. Although straightforward and potentially effective, such a parameter optimization design approach is generally suboptimal when compared to nonlinear time-varying controllers. In order to get a clear insight how far from optimal the parameter optimized controller is, it would be beneficial to apply advanced numerical techniques of finding optimal trajectories of nonlinear system control variables. Other benefits of using the nonlinear open-loop optimization include (i) assessment on the degree of GCC improvement achieved by introducing different actuators and (ii) gaining an insight on how the state controller can be extended by feedforward and/or gain scheduling actions to improve the performance.

Any automotive control system that includes many, especially redundant actuators is a good candidate for applying control variable optimization. This includes advanced engine control systems (Kolmanovsky, 2001), hybrid vehicle controls (Sundstroem and Stefanopoulou, 2006), and vehicle dynamics control systems (Velenis and Tsiotras, 2005; Hattori *et al*., 2005).

A traditional way of solving the control variable optimization problem includes complete time-discretization of the problem and its conversion into a nonlinear programming formulation (Betts, 2001). The penalty functions related to the state and control variable constraints, and also plant equation constraints are added to the cost function. The control and state variables can, thus, be treated as independent variables, so that the cost function gradient calculation is relatively simple. However, the optimization problem formulated in such a way can be characterized by a slow convergence due to additional plant equations equality constraints. Also, numerical stability can be sensitive to choice of various optimization parameters such as discretization period, weighting factors of penalty functions etc.

In this paper we present a GCC optimization approach based on the nonlinear optimization method developed in (Kasac, 1998). In contrast to the nonlinear programming approach, the plant equations constraints are not included in the cost function. The control and state variables are rather treated as dependent variables (coupled via plant equations), so that the final algorithm has a backward-in-time structure similar to the backpropagation-through-time (BPTT) algorithm (Werbos, 1990), which is mostly used as a learning algorithm for recurrent neural networks. Such an exact gradient algorithm is more complex than the nonlinear programming-based algorithm, but it can provide better and numerically more stable convergence properties. GCC application of the algorithm is illustrated on an example of double lane change maneuver executed by using control actions of active rear steering and active rear differential actuators.

2. OPTIMAL CONTROL ALGORITHM

2.1 Continuous-Time Problem Formulation

A continuous-time nonlinear optimal control problem is considered. The problem is to find the control vector $\mathbf{u}(t)$ that minimizes the cost function

$$J_0 = \int_0^{t_f} \bar{F}\left(\mathbf{x}(t), \mathbf{u}(t)\right) dt, \tag{1}$$

subject to the nonlinear continuous-time plant equations

$$\dot{\mathbf{x}}(t) = \boldsymbol{\phi}(\mathbf{x}(t), \mathbf{u}(t)), \tag{2}$$

and the initial and final conditions of the state vector

$$\mathbf{x}(0) = \mathbf{x}_0, \quad \mathbf{x}(t_f) = \mathbf{x}_f, \tag{3}$$

then subject to the control and state vector inequality constraints

$$\mathbf{g}\left(\mathbf{x}(t), \mathbf{u}(t)\right) \geq 0, \tag{4}$$

and equality constraints

$$\mathbf{h}\left(\mathbf{x}(t), \mathbf{u}(t)\right) = 0, \tag{5}$$

where $\mathbf{x}(t)$ is the n-dimensional state vector, $\mathbf{u}(t)$ is the m-dimensional control vector, $\mathbf{g}(\mathbf{x}(t), \mathbf{u}(t))$ is the p-dimensional vector function of inequality constraints, $\mathbf{h}(\mathbf{x}(t), \mathbf{u}(t))$ is the q-dimensional vector function of equality constraints, and t_f is the terminal time.

2.2 Discrete-Time Problem Formulation

The discrete-time form of the cost function (1) reads

$$J_0 = \tau \sum_{i=0}^{N-1} \bar{F}(\mathbf{x}(i), \mathbf{u}(i)), \tag{6}$$

where N is the number of sampling intervals, $\tau = t_f / N$ is the sampling interval, and $\mathbf{x}(i)$ and $\mathbf{u}(i)$ are the state and control vectors in the i-th time interval $t_i = i\tau$, i=0, 1,…, N-1, respectively. The set of differential equations (2) is transformed to the set of difference equations

$$\mathbf{x}(i+1) = \mathbf{f}\left(\mathbf{x}(i), \mathbf{u}(i)\right), \tag{7}$$

where the Euler discretization method[1] is used

$$\mathbf{f}(\mathbf{x}(i), \mathbf{u}(i)) = \mathbf{x}(i) + \tau \boldsymbol{\phi}(\mathbf{x}(i), \mathbf{u}(i)). \tag{8}$$

The initial and final conditions of the state vector are

$$\mathbf{x}(0) = \mathbf{x}_0, \quad \mathbf{x}(N) = \mathbf{x}_f, \tag{9}$$

and the control and state vector inequality and equality constraints read

$$\mathbf{g}\left(\mathbf{x}(i), \mathbf{u}(i)\right) \geq 0, \tag{10}$$

$$\mathbf{h}\left(\mathbf{x}(i), \mathbf{u}(i)\right) = 0. \tag{11}$$

2.3 Penalty Method Approach

The next problem-formulation step includes expansion of the cost function (6) with penalty functions for constraints:

$$J = J_0 + J_1 + J_2 + J_3, \tag{12}$$

where

$$J_1 = K_B \sum_{k=1}^{n} \left(\mathbf{x}_k(N) - \mathbf{x}_k(t_f)\right)^2, \tag{13}$$

is the penalty function for the final boundary conditions (9), K_B is the weighting coefficient of the penalty function, and $\mathbf{x}_k(t_f)$ is the k-th component of the state vector at the terminal time t_f.

Further,

$$J_2 = \bar{K}_V \sum_{i=0}^{N-1} \sum_{k=1}^{N_p} g_k^2\left(\mathbf{x}(i), \mathbf{u}(i)\right) H^-\left(g_k\left(\mathbf{x}(i), \mathbf{u}(i)\right)\right), \tag{14}$$

is the penalty function for inequality constraints (10), where $H^-(x)$ is the Heaviside step function defined as

$$H^-(x) = \begin{cases} 0, & \text{if} \quad x \geq 0, \\ 1, & \text{if} \quad x < 0, \end{cases}$$

and $\bar{K}_V$ is the penalty function weighting coefficient for inequality constraints. Finally, the penalty function for the equality constraints (11) is given by

$$J_3 = \bar{K}_E \sum_{i=0}^{N-1} \sum_{k=1}^{N_q} h_k^2\left(\mathbf{x}(i), \mathbf{u}(i)\right), \tag{15}$$

where $\bar{K}_E$ is the corresponding weighting coefficient.

By setting $\bar{K}_V = \tau K_V$ and $\bar{K}_E = \tau K_E$, the equation (12) can be expressed as

$$J = \tau \sum_{i=0}^{N-1} F\left(\mathbf{x}(i), \mathbf{u}(i)\right) + K_B \sum_{k=1}^{n} \left(x_k(N) - x_k(t_f)\right)^2, \tag{16}$$

where

$$F\left(\mathbf{x}(i), \mathbf{u}(i)\right) = \bar{F}\left(\mathbf{x}(i), \mathbf{u}(i)\right) + K_E \sum_{k=1}^{N_q} h_k^2\left(\mathbf{x}(i), \mathbf{u}(i)\right) + \\ + K_V \sum_{k=1}^{N_p} g_k^2\left(\mathbf{x}(i), \mathbf{u}(i)\right) H^-\left(g_k\left(\mathbf{x}(i), \mathbf{u}(i)\right)\right). \tag{17}$$

Hence, the optimal control problem (6) to (11) can be formulated in the following form

$$J = \tau \sum_{i=0}^{N-1} F\left(\mathbf{x}(i), \mathbf{u}(i)\right) + J_1, \tag{18}$$

$$\mathbf{x}(i+1) = \mathbf{f}\left(\mathbf{x}(i), \mathbf{u}(i)\right), \quad \mathbf{x}(0) = \mathbf{x}_0. \tag{19}$$

2.4 Gradient Optimization Method

The gradient descent algorithm with respect to control vector $\mathbf{u}(i)$ is given by:

$$\mathbf{u}^{(l+1)}(i) = \mathbf{u}^{(l)}(i) - \eta \mathbf{J}_u(i), \qquad \mathbf{J}_u(i) = \frac{\partial J}{\partial \mathbf{u}^{(l)}(i)}, \tag{20}$$

where l = 1, 2, …, M. The index l denotes the l-th iteration of the gradient algorithm, M is the number of iterations, and η is the convergence coefficient.

The gradient of the cost function (18) in the l-th iteration of the gradient algorithm and i-th sampling interval is

$$\frac{\partial J}{\partial u_k(j)} = \tau \sum_{i=0}^{N-1} \frac{\partial F(i)}{\partial u_k(j)} + \frac{\partial J_1}{\partial u_k(j)}, \tag{21}$$

where $F(i) \equiv F\left(\mathbf{x}(i), \mathbf{u}(i)\right)$, and k = 1, 2, …, m.

The sum on the right-hand side of (21) can be evaluated as follows

$$\tau \sum_{i=0}^{N-1} \frac{\partial F(i)}{\partial u_k(j)} = \tau \frac{\partial F(j)}{\partial u_k(j)} + \tau \sum_{i=j+1}^{N-1} \frac{\partial F(i)}{\partial u_k(j)}, \tag{22}$$

where the terms for $i < j$ are equal to zero, because the state vector $\mathbf{x}(i)$ is not dependent on $\mathbf{u}(j)$ for $j > i$ (the causality principle: the state vector in the past is not dependent on control vector in the future).

The terms in the sum on the right-hand side of (22) depend on $u_k(j)$ implicitly through $\mathbf{x}(i)$ for $i > j$, which gives

[1] Since the proposed algorithm is found to be robust with respect to the choice of number of time intervals N, we use the simple Euler method with the sampling interval τ selected to a value that is small enough to provide satisfactory accuracy of optimization.

$$\frac{\partial F(i)}{\partial u_k(j)} = \sum_{r=1}^{n} \frac{\partial F(i)}{\partial x_r(i)} \frac{\partial x_r(i)}{\partial u_k(j)}. \quad (23)$$

The following step is calculation of the partial derivative term $\partial x_r(i)/\partial u_k(j)$ in (23). Based on (19), the chain rule for ordered derivatives is obtained:

$$\frac{\partial x_r(j+1)}{\partial u_k(j)} = \frac{\partial f_r(j)}{\partial u_k(j)}, \quad (24)$$

$$\frac{\partial x_r(i)}{\partial u_k(j)} = \sum_{p=1}^{n} \frac{\partial f_r(i-1)}{\partial x_p(i-1)} \frac{\partial x_p(i-1)}{\partial u_k(j)}, \quad (25)$$

for $i = j+2, \ldots, N-1$, where $f_r(j) \equiv f_r(\mathbf{x}(j), \mathbf{u}(j))$.

If the second term on the right-hand side of the expression (21) is denoted as

$$S_k(j) = \sum_{i=j+1}^{N-1} \frac{\partial F(i)}{\partial u_k(j)}, \quad (26)$$

then the following recurrent algorithm for the calculation of the sum (23) can be obtained

$$P_r(N-1) = 0, \quad (27)$$

$$P_r(j) = \frac{\partial F(j+1)}{\partial x_r(j+1)} + \sum_{l=1}^{n} P_l(j+1) \frac{\partial f_l(j+1)}{\partial x_r(j+1)}, \quad (28)$$

$$S_k(j) = \sum_{r=1}^{n} \frac{\partial f_r(j)}{\partial u_k(j)} P_r(j), \quad (29)$$

where $j = N-2, N-3, \ldots, 0$; $r = 1, 2, \ldots, n$; $k = 1, 2, \ldots, m$. Detailed derivation of the backward-in-time recurrent algorithm (27)-(29), as well as the gradient $\partial J_1 / \partial u_k(j)$, is provided in (Kasac, 1998).

The standard gradient algorithm with the constant convergence coefficient η and a linear gradient $\mathbf{J}_u$ is characterized by a slow convergence. Small value of the gradient $\mathbf{J}_u$ near the optimal solution is the main reason for the slow convergence. In this work we use a simple "sliding-mode"-based modification of the gradient algorithm, where the linear dependence on $\mathbf{J}_u$ is replaced by the following nonlinear form:

$$\mathbf{u}^{(l+1)}(i) = \mathbf{u}^{(l)}(i) - \eta \frac{\mathbf{J}_u(i)}{\varepsilon + \|\mathbf{J}_u(i)\|}, \quad (30)$$

where

$$\|\mathbf{J}_u\| = \sqrt{\sum_{i=1}^{N-1} \mathbf{J}_u^T(i) \cdot \mathbf{J}_u(i)}, \quad (31)$$

and ε is a positive small parameter. Such a nonlinear modification of the gradient algorithm provides a stronger influence of the gradient $\mathbf{J}_u$ near the optimal solution, and consequently better convergence.

3. VEHICLE DYNAMICS MODEL

The 10 degree of freedom (DOF) vehicle dynamics model (Hancock, 2006) is adapted in this report, in order to get a simpler and still relatively accurate model structure convenient for control variable optimization. The simplification primarily relates to omitting the roll, pitch, and heave DOF.

3.1 State-Space Subsystem

The considered vehicle dynamics model include three state variables related to longitudinal, lateral and yaw DOF, three state variables related to vehicle trajectory in the inertial coordinate system, four state variables corresponding to the rotational speeds of each wheel, first order dynamics of the tire load subsystem, and first order dynamics of rear steering and rear differential actuators.

The differential equations for the each subsystem are given as follows.

1) *Longitudinal, lateral, and yaw DOF*:

$$\dot{U} = Vr + \frac{1}{M}(F_{x1} + F_{x2} + F_{x3} + F_{x4}), \quad (32)$$

$$\dot{V} = -Ur + \frac{1}{M}(F_{y1} + F_{y2} + F_{y3} + F_{y4}), \quad (33)$$

$$\dot{r} = \frac{b}{I_{zz}}(F_{y1} + F_{y2}) - \frac{c}{I_{zz}}(F_{y3} + F_{y4}) - \frac{t}{2I_{zz}}(F_{x1} + F_{x3}) + \frac{t}{2I_{zz}}(F_{x2} + F_{x4}), \quad (34)$$

$$\dot{\psi} = r, \quad (35)$$

$$\dot{X} = U\cos\psi - V\sin\psi, \quad (36)$$

$$\dot{Y} = U\sin\psi + V\cos\psi, \quad (37)$$

where U and V are the longitudinal and lateral velocity, r is the yaw rate, X and Y define the vehicle position in the inertial coordinate system, and ψ is the yaw angle. Further, F_{xi} and F_{yi}, i=1, 2, 3, 4, are the longitudinal and lateral forces of the i-th tire in the vehicle coordinate system (i=1, 2 – front tires; i=1, 3 – left tires), M is the vehicle mass, I_{zz} is the vehicle moment of inertia around the vertical axis, b is the longitudinal distance from the front axle to the vehicle centre of gravity (CoG), c is the longitudinal distance from the rear axle to the CoG, and t is the track.

2) *The wheel rotational dynamics*:

$$\dot{\omega}_i = \frac{1}{I_{wi}} T_i - \frac{R}{I_{wi}} F_{xti}, \quad (38)$$

where ω_i is the rotational speed of the i-th wheel, F_{xti} is the longitudinal force of the i-th tire in the tire coordinate system, T_i is the torque at the i-th wheel, I_{wi} is the wheel moment of inertia, and R is the effective tire radius.

3) *Delayed total lateral force (needed to calculate the lateral tire load shift)*:

$$\dot{F}_{y\Sigma d} = -\frac{1}{\tau_d} F_{y\Sigma d} + \frac{1}{\tau_d}(F_{y1} + F_{y2} + F_{y3} + F_{y4}), \quad (39)$$

where τ_d is the time constant that is chosen to provide a good fit of 10 DOF model lateral tire load shift behavior.

4) *The actuator dynamics*:

$$\dot{\delta}_r = -\frac{1}{\tau_\delta} \delta_r + \frac{1}{\tau_\delta} \bar{\delta}_r, \quad (40)$$

$$\frac{d\Delta T_r}{dt} = -\frac{1}{\tau_T} \Delta T_r + \frac{1}{\tau_T} \Delta \bar{T}_r, \quad (41)$$

where δ_r is the rear wheel steering angle, ΔT_r is the rear differential torque shift, and τ_δ and τ_T are the actuator time constants.

3.2 Longitudinal Slip Subsystem

The longitudinal tire slip is given by

$$\eta_i = \frac{R\omega_i - U_i}{U_i}, \tag{42}$$

where U_i is the longitudinal velocity of the vehicle body at corner *i*:

$$U_{1,3} = U - \frac{t}{2}r, \qquad U_{2,4} = U + \frac{t}{2}r. \tag{43}$$

3.3 Lateral Slip Subsystem

The tire slip angle is calculated as

$$\alpha_i = \delta_i - \arctan\frac{V_i}{U_i}, \tag{44}$$

where δ_i is the road wheel angle, and V_i is the lateral velocity of the vehicle body at the corner *i*:

$$V_{1,2} = V + br, \qquad V_{3,4} = V - cr. \tag{45}$$

Note that in this work $\delta_1 = \delta_2$ are considered to be external (driver's) input variables, and $\delta_3 = \delta_4$ are control inputs to be optimized (active rear steering).

3.4 Tire Load Subsystem

In the absence of heave dynamics, the tire load of each tire may be calculated as:

$$F_{z1,2} = \frac{1}{2}\left(\frac{cMg}{l} \mp \frac{h_g}{t}F_{y\Sigma d}\right), \quad F_{z3,4} = \frac{1}{2}\left(\frac{bMg}{l} \mp \frac{h_g}{t}F_{y\Sigma d}\right), \tag{46}$$

where *l* is the wheelbase and h_g is the CoG height. Note that the second term corresponds to the lateral load shift, where $F_{y\Sigma d}$ is given by (39). The longitudinal tire load shift is neglected in this study.

3.5 Tire Subsystem

The tire model is based on a simplified form of Magic formula model (Bakker *et al.*, 1987). The simplification leads to a significant reduction of complexity of analytical Jacobian matrices in (28) and (29), which is primarily determined by the tire model complexity. The longitudinal and lateral tire forces are calculated as static functions of the longitudinal slip, lateral slip, and normal loads to tires:

$$s_i = \sqrt{\eta_i^2 + \alpha_i^2}, \tag{47}$$

$$F_i = \mu F_{zi} D \sin\left(C \arctan\left(kBs_i\right)\right), \tag{48}$$

$$F_{xti} = \frac{\eta_i}{s_i}F_i, \qquad F_{yti} = \frac{\alpha_i}{s_i}F_i, \tag{49}$$

where μ is the tire friction coefficient, *B*, *C* and *D* are tire model parameters, and $k = 180/\pi$. The above tire model predicts the friction circle as a basic tire property.

The calculated tire forces are then transformed to the chassis coordinate system to serve as inputs of the state-space subsystem (Subsection 3.1) and the tire load subsystem (Subsection 3.4):

$$\begin{aligned} F_{xi} &= F_{xti}\cos\delta_i - F_{yti}\sin\delta_i \\ F_{yi} &= F_{xti}\sin\delta_i + F_{yti}\cos\delta_i \end{aligned}. \tag{50}$$

3.6 Rear Active Differential Subsystem

The torque at each wheel is given by

$$T_{1,2} = -\frac{T_b}{4}, \qquad T_{3,4} = \frac{T_i}{2} \mp \Delta T_r - \frac{T_b}{4}, \tag{51}$$

where ΔT_r is the differential torque shift control variable, T_i is the input torque (driveline torque) and T_b is the braking torque (equally distributed braking force to each wheel is assumed).

The differential torque shift ΔT_r is subject to constraints related to the left and right wheel speed difference (Hancock, 2006):

(a) Active limited-slip differential (ALSD):

$$\omega_3 > \omega_4 \Rightarrow \Delta T_r > 0, \quad \omega_3 < \omega_4 \Rightarrow \Delta T_r < 0\,.$$

(b) Torque vectoring differential (TVD):

$$\omega_4 < k_{AWSD}\omega_3 \Rightarrow \Delta T_r > 0, \quad \omega_3 < k_{AWSD}\omega_4 \Rightarrow \Delta T_r < 0\,,$$

where k_{AWSD}>1 is the allowable wheel speed difference factor (for a realistic TVD $k_{AWSD} \approx 1.25$). Note that k_{AWSD}=1 for the ALSD. The above-mentioned constraint is included in plant model as

$$\Delta\bar{T}_r = H^+\left(w_1\right)H^+\left(\Delta T_r\right)\Delta T_r + H^-\left(w_2\right)H^-\left(\Delta T_r\right)\Delta T_r, \tag{52}$$

where $w_1 = k_{AWSD}\omega_3 - \omega_4$, $w_2 = \omega_3 - k_{AWSD}\omega_4$, and $H^-(x)$ and $H^+(x) = 1 - H^-(x)$ are Heaviside step functions (Section 2).

4. OPTIMAL CONTROL PROBLEM FORMULATION

The optimal control objectives is to find the control variables which ensure that vehicle follows the reference trajectory in *X-Y* inertial coordinate system with a minimum tracking error. In other words, the problem is to find the rear steering angle δ_r and/or the rear differential torque shift ΔT_r which minimize the cost function:

$$J = K_s\int_0^{t_f}\left[(X_R - X)^2 + (Y_R - Y)^2\right]dt + \sum_{i=1}^{2}K_{ui}\int_0^{t_f}\frac{u_i^2}{U_{i\max}^2}dt, \tag{53}$$

where X_R and Y_R are coordinates of the reference trajectory, $u_1 \equiv \delta_r$, $u_2 \equiv \Delta T_r$, $U_{1\max} \equiv \delta_{r\max} = 20^\circ$, $U_{2\max} \equiv \Delta T_{r\max} = 1250\,\mathrm{Nm}$, and K_s and $K_{u1,2}$ are weighting factors of individual cost functions.

Also, the following inequality constraints of the control and state variables can be considered and realized through the penalty cost function (14):

a) Control variables constraints:

$$\left|\Delta T_r\right| \le \Delta T_{r\max} = 1250\,\mathrm{Nm}, \qquad \left|\delta_r\right| \le \delta_{r\max} = 20^\circ, \tag{54}$$

b) Limit of vehicle side slip angle:

$$\left|\beta\right| \le \beta_{\max} \approx 5^\circ, \qquad \beta = \arctan\frac{V}{U}. \tag{55}$$

The functionality of the optimal control method for the above formulation has been fully verified on examples of step steer and double lane change maneuvers with different constraints and friction coefficients μ. Section 5 presents the results for double lane change maneuver with no constraints on the side slip angle β. The reference trajectory is of Gaussian type, and is given by red dashed line in Figs. 1-5. The optimization is subject to the following equality constraints (boundary constraints, cf. (13)) on the final trajectory point:

$$Y(t_f) = Y(0), \qquad dY(t_f)/dt = 0. \tag{56}$$

5. OPTIMIZATION RESULTS

The C code optimization program for the double lane change example is executed on a personal computer with Intel Pentium 4 processor (3.20 GHz). The terminal time is t_f=6 s, the sampling interval is τ =0.003 s, so that the number of time intervals is N=2000. The number of iterations of the gradient algorithm is M=6000. The initial value of the control vector (for the initialization of the gradient algorithm) is set to zero. The execution time is typically in the range of several minutes.

Fig. 1 shows the results of optimization of the front road wheel angle δ_f for asphalt road (μ=1), with the aim to reach the desired vehicle trajectory. That is, the optimization task is to find an ideal driver steering input referred to the road wheel angle. The results in Fig. 1 illustrate that the desired, relatively sharp vehicle trajectory cannot be fully satisfied by using the front wheel steering at the given velocity of 22 m/s. The maximum absolute value of the lateral acceleration reaches about $a_y = \dot{V} + Ur = 6.5\,\mathrm{m/s^2} \cong 0.65g$.

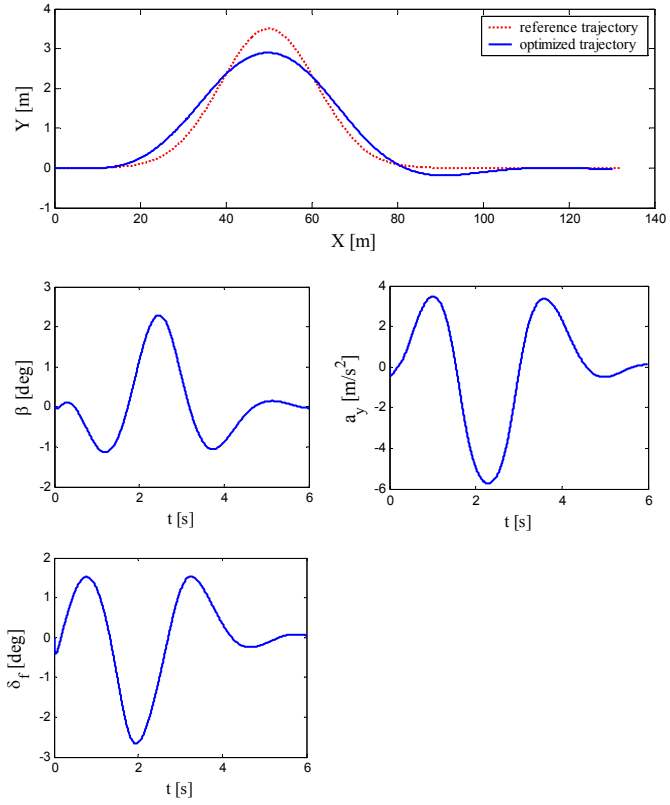

Fig. 1. Front wheel steering optimization results for asphalt road (μ = 1).

Figs. 2-5 shows the optimization results for a road condition characterized by the tire-road friction coefficient μ = 0.6 (e.g. wet asphalt surface) for different vehicle dynamics actuators: active rear steering (ARS), active torque vectoring differential (TVD), active limited-slip differential (ALSD), and combined ARS and TVD. The top plot of each figure include three trajectories: (i) reference trajectory that corresponds to the optimized (reached) trajectory for μ = 1 in Fig. 1, (ii) trajectory when no control action is used (δ_r = 0, ΔT_r = 0), and (iii) trajectory reached by using the control action. The front steering input is taken from Fig. 1 (no driver model is used).

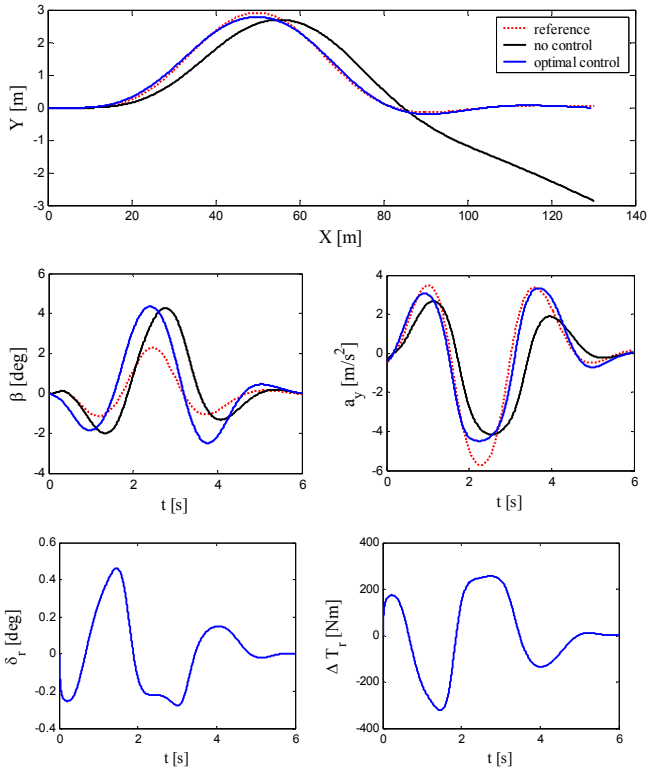

Fig. 2. Optimization results for ARS+TVD control and μ = 0.6.

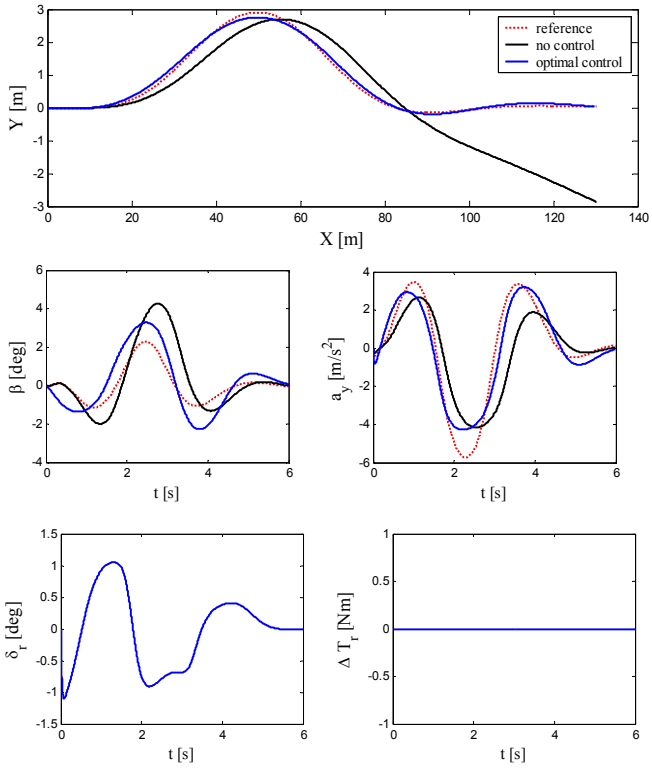

Fig. 3. Optimization results for ARS control and μ = 0.6.

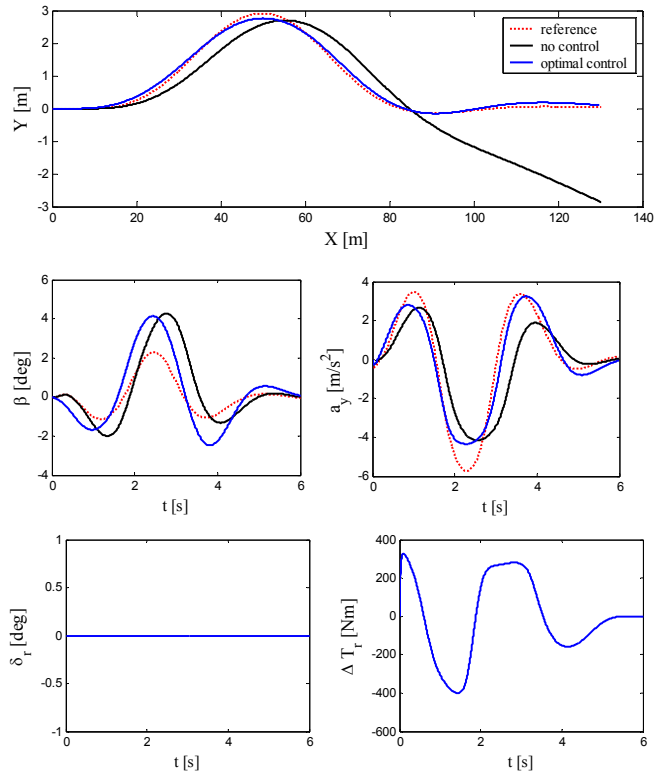

Fig. 4. Optimization results for TVD control and $\mu = 0.6$.

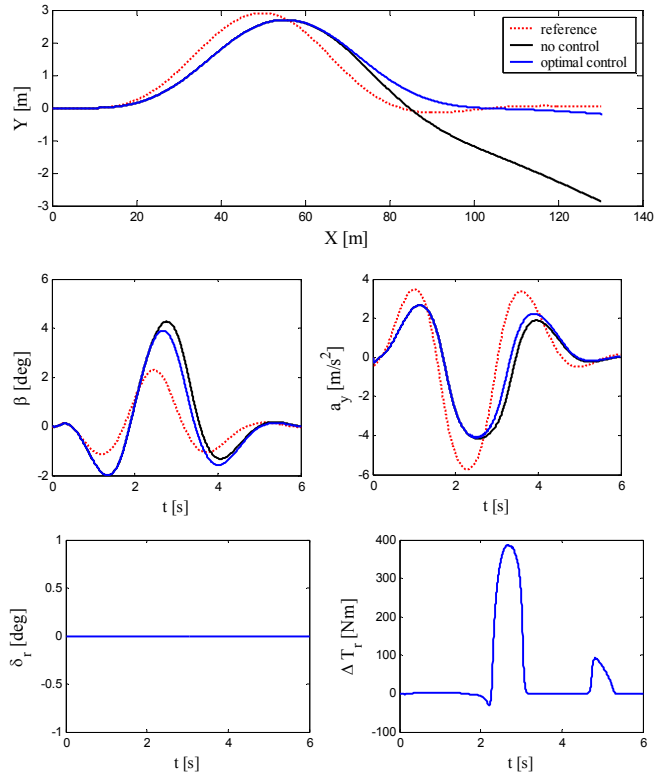

Fig. 5. Optimization results for ALSD control and $\mu = 0.6$.

Since the reference lateral acceleration $a_y \cong 6.5\,\mathrm{m/s^2}$ is close to be achievable on the road with $\mu = 0.6$, the optimization of combined ARS+TVD control variables result in accurate trajectory following (Fig. 2). In the case of individual ARS or TVD control, the trajectory following accuracy remains almost the same as in the case of combined ARS+TVD control (cf. Figs. 3-4 and Fig. 2). The main difference is that the individual controls require larger magnitudes of the control inputs δ_r and ΔT_r than the combined control. When comparing the two individual controls, it is important to note that the ARS control provokes smaller magnitudes of the vehicle side slip angle β than the TVD control. The active limited slip differential (ALSD) cannot compensate for the understeer behavior in the first part of maneuver, and the corresponding trajectory error is the same as for the passive vehicle (Fig. 5). This is because the ALSD cannot generate oversteer, i.e. it can only shift torque to the slower/inner wheel (understeer generation; cf. Subsection 3.6). Similar comparative performance has been obtained for lower μ values as well.

6. CONCLUSIONS

A back-propagation-through-time (BPTT) exact gradient method of optimal control has been applied for control variable optimization in Global Chassis Control systems. The optimization approach has been illustrated on an example of double lane change maneuver. The approach is proven to be numerically robust and precise, and it can give valuable insights into the ultimate GCC performance. The future work will be directed to use of the developed optimization method for various multi-input GCC optimization studies. Further improvements of the optimization method in terms of using more precise vehicle dynamics model, numerical calculation of Jacobian matrices, and enhanced optimization algorithm will be considered as well.

REFERENCES

Bakker, E., Nyborg, L., Pacejka, H. B. (1987). Tyre Modelling for Use in Vehicle dynamics Studies. *SAE paper 870421*.

Betts, J. T. (2001). *Practical Methods for Optimal Control using Nonlinear Programming.* Society of Industrial and Applied Mathematics, Philadelphia, PA.

Hancock, M. (2006). *Vehicle Handling Control using Active Differentials*, Ph.D. Thesis, University of Loughborough, UK.

Hattori, Y., Ono, E., Hosoe, S., Tanaka, T. (2005). Optimum Vehicle Trajectory Control for Obstacle Avoidance Problem. *IEEE Int. Symposium on Industrial Electronics*, Vol. I, pp. 367-372, Dubrovnik, Croatia.

Kasac, J. (1998). *Optimal Control of Nonlinear Systems using Neural Networks*, Master Thesis (in Croatian), University of Zagreb, Croatia.

Kolmanovsky, I. V. (2001). Optimal Control Techniques for Assessing Feasibility and Defining Subsystem Level Requirements: An Automotive Case Study. *IEEE Trans. on Control System Technology*, Vol. 9, No. 3, pp. 524-534.

Sundstroem, O., Stefanopoulou, A. (2006). Optimal Power Split in Fuel Cell Hybrid Electric Vehicle with different Battery Sizes, Drive cycles, and Objectives. *IEEE Conference on Control Applications*, Munich.

Velenis, E. and Tsiotras P. (2005). Minimum Time vs. Maximum Exit Velocity Path Optimization During Cornering. *IEEE Int. Symposium on Industrial Electronics*, Vol. I, pp. 355-360, Dubrovnik, Croatia.

Werbos, P.J. (1990). Backpropagation through time: What it does how to do it. *Proceedings of the IEEE*, vol. 78, no. 10, pp. 1550-1560.